

MICROCOPY RESOLUTION TEST CHART
NATIONAL BUREAU OF STANDARDS-1963-A

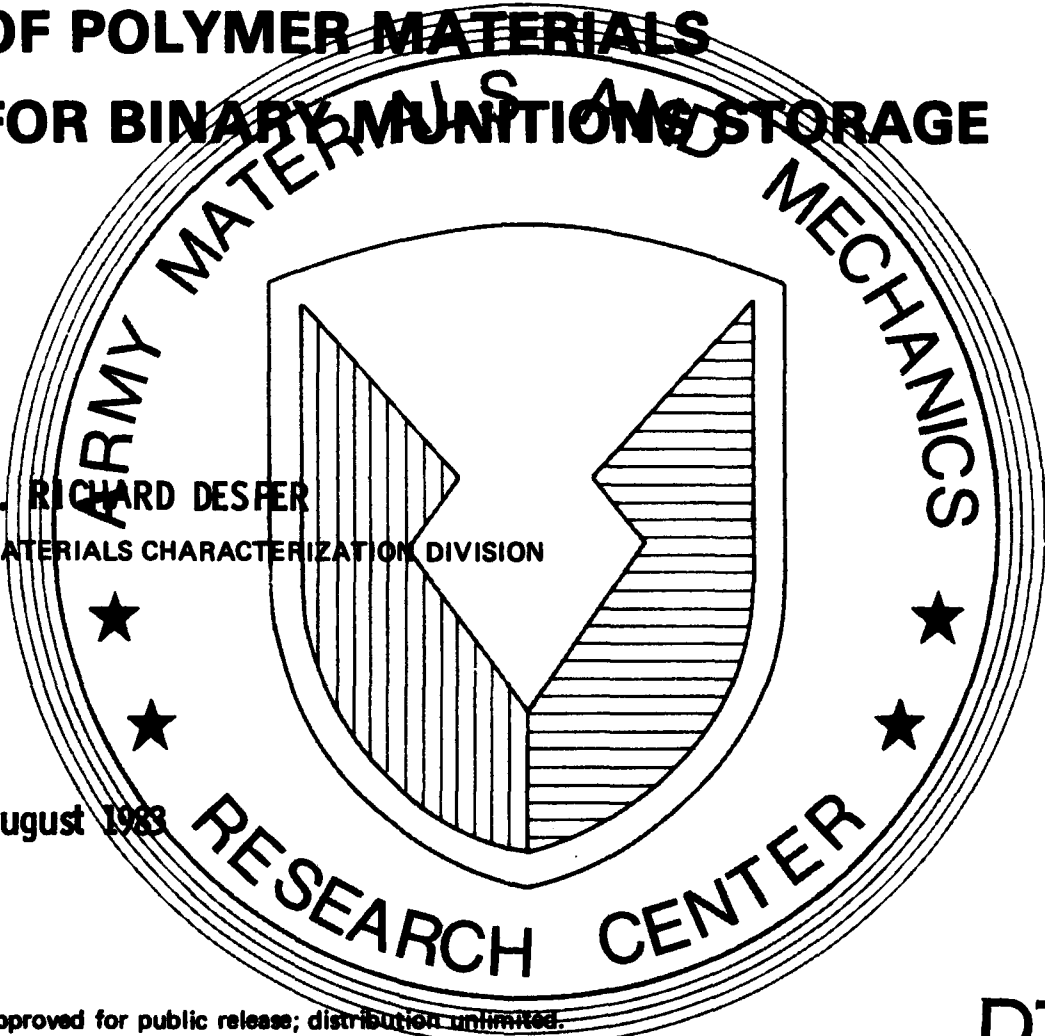
AMMRC TR 83-45

AD



CHARACTERIZATION AND SELECTION OF POLYMER MATERIALS FOR BINARY MUNITIONS STORAGE

ADA132428



C. RICHARD DESFER
MATERIALS CHARACTERIZATION DIVISION

August 1983

Approved for public release; distribution unlimited.

ARMY MATERIALS AND MECHANICS RESEARCH CENTER
Watertown, Massachusetts 02172

DTIC
ELECTE
SEP 15 1983
S D

DTIC FILE COPY

83 09 13 041

The findings in this report are not to be construed as an official Department of the Army position, unless so designated by other authorized documents.

Mention of any trade names or manufacturers in this report shall not be construed as advertising nor as an official indorsement or approval of such products or companies by the United States Government.

DISPOSITION INSTRUCTIONS

Destroy this report when it is no longer needed.
Do not return it to the originator.

UNCLASSIFIED

SECURITY CLASSIFICATION OF THIS PAGE(When Data Entered)

Block No. 20

ABSTRACT

→ The purpose of this study was to investigate the materials properties required for storage of DF (methylphosphonic difluoride) over extended periods of time at temperatures as high as 70°C, anticipating more severe environmental requirements. Specimens of nominally 96/4 ethylene/propylene copolymer were examined by SEM, GPC, FTSIR, X-ray diffraction, and tensile testing. Specimens fabricated into containers and exposed to DF for eight years were compared to control samples of the same vintage and to newly processed polymer sheets of the same resin type. The molecular weight distributions were broad, with M_w values of 160,000 to 170,000 and M_n values of 24,000 to 30,000. These values were unaffected by exposure to DF with the exception of the interior sidewall, which had been in contact with liquid DF and showed a narrow surface layer of discolored cross-linked material. X-ray diffraction showed the expected 60% crystallinity, but also revealed a pattern of residual stress. However, no loss in mechanical properties was observed. The environmental stress cracking process is the major factor contributing to premature failure in DF containers, with polymer oxidation playing only a secondary role. Materials and processing factors affecting performance are discussed. Further work continues in this area. ←

UNCLASSIFIED

SECURITY CLASSIFICATION OF THIS PAGE(When Data Entered)

CONTENTS

	Page
INTRODUCTION.	1
Samples.	1
Experimental	1
Results	
Preliminary Inspection and Microscopic Examination.	3
Gel Permeation Chromatography	7
Mechanical Properties	10
X-Ray Diffraction	12
X-Ray Fluorescence.	17
Infrared Absorption	18
DISCUSSION.	22
RECOMMENDATIONS	25
ACKNOWLEDGMENTS	26

Accession For	
NTIS GRA&I	<input checked="" type="checkbox"/>
DTIC TAB	<input type="checkbox"/>
Unannounced	<input type="checkbox"/>
Justification	
By _____	
Distribution/ _____	
Availability Codes	
_____ and for _____	
Dist _____	_____
A	



INTRODUCTION

The purpose of this study is to investigate the materials properties required for the storage of DF (methylphosphonic difluoride) over extended periods of time at elevated temperatures. Since the current polyethylene container has been found capable of meeting the more limited present requirements, it has been used as a starting point for evaluating baseline materials requirements. The present project is focused primarily on the thermoplastic polyolefins, although other polymeric materials may be examined on an exploratory basis.

Samples

Samples of DF container material were made available for comparative characterization. Two different polymer thicknesses are used in the container design: the side walls and one end wall are 1/4 inch thick, or approximately 6 mm, while the remaining end wall is 1/16 inch thick, or 1.5 mm. The 1.5-mm end is called the burst plate, while the 6-mm end, through which liquid is introduced and where the final seal is effected, will be called the plug end. The cylindrical container is fabricated from extruded pipe stock for the sidewalls and flat sheet stock for the ends.

The specimens are divided into three classes: 1) OLD - sheet stock (1.5 mm and 6 mm) from 1973 production runs; 2) NEW - sheet stock (1.5 mm and 6 mm) from 1977 production runs; and 3) EXPOSED - two canisters (labelled no. 317 and no. 318) which were manufactured and filled with DF in November-December 1973. These canisters were opened and drained in 1981.

The specimens will be designated by their class and thickness; e.g., OLD - 1.5 mm and NEW - 6 mm. Where appropriate, the particular location being sampled will be indicated. Thus, for the EXPOSED - 6-mm specimens, either plug end or sidewall will be specified.

The material, in all cases, is reported to be a copolymer of ethylene and butene-1; the ethylene being the major constituent. Presumably, the minor butene-1 constituent polymerizes to leave ethyl side groups pendent on a largely linear polyethylene molecule. The result is often termed a medium density polyethylene of density 0.94 g/cm^3 , intermediate in density between the strictly linear high density grades, and the low density grades possessing extensive long-chain branching.

Experimental

Molecular weight characterization was accomplished using the Waters Model 150-C Gel Permeation Chromatograph. The polymer specimens were dissolved in trichlorobenzene (TCB) and run at 135°C . Five chromatograms were obtained for each sample solution. Data were analyzed against known calibration standards using an on-line microprocessor.

Tension tests were run on an Instron Tensile Tester by ASTM procedure D638. Specimen Type V was used, which required a total sample length of only 2.5 inches, since certain samples were available only as 4.75-inch-diameter disks. Ten specimens were tested; five in the machine direction and five in the transverse direction. The cross section of each specimen was gauged by a micrometer prior to testing.

Elastic modulus data were measured using an H. M. Morgan Model PPM-5 dynamic modulus tester, following ASTM F89-68. A single density value of 0.942 g/cm³ was used to calculate the elastic modulus from the sonic velocity values measured by this method.

X-ray diffraction patterns were obtained using a Polaroid XR-7 cassette at a nominal 3-cm working distance, using nickel-filtered radiation from a copper anode tube of wavelength 1.5418 Å. The exact working distance was determined using nickel foil as a reference material.

Quantitative X-ray diffraction data were obtained using a North American Phillips wide angle goniometer, type 42202, also using copper anode radiation filtered by nickel foil. Intensity values were measured by pulse counting at a series of Bragg angle values by a motor-driven step scanner under minicomputer control.¹ Data were obtained using both the symmetrical reflection mode and the symmetrical transmission mode as described by Wilchinsky.² The significance of the two modes of operation will be discussed in greater detail elsewhere in this report. Data were obtained in the range of $2\theta = 8^\circ$ to 40° . Subsequently, the pattern between $2\theta = 13^\circ$ and 29° was resolved mathematically into one amorphous, and two strong crystal reflections, the 110 and 200 planes, using Gaussian line shapes and a least-squares procedure.³ Crystallinity values were calculated from the relative areas $A_{\text{amorphous}}$, A_{110} and A_{200} following the method of Gopalan and Mandelkern:⁴

$$X_c = (A_{110} + A_{200}) / (A_{110} + A_{200} + A_{\text{amorphous}}). \quad (1)$$

As the data were processed, evidence of residual stress appeared in the transmission diffraction patterns. Definite shoulders appeared on the low angle sides of the 110 and 200 crystal peaks, arising from material under significant tensile strain. The peak and shoulder portions were readily resolved into separate peaks of Gaussian shape.

$$I = I_0 \exp \left\{ - \left[1.666(2\theta - 2\theta_0) / \beta \right]^2 \right\} \quad (2)$$

where $2\theta_0$ is the center position of a given component and β is the line width at half-peak intensity. The crystal strain ϵ is calculated from the separation $\Delta(2\theta)$ between peak and shoulder components using the following formula:

$$\epsilon = \Delta(2\theta) / (114.59 \tan \theta) \quad (3)$$

(see Reference 5; the above form of the equation uses 2θ expressed in degrees rather than radians). The shoulder on the low angle side represents crystals in tension, since lower Bragg angles correspond to larger spacings. The fraction under tension f_t has been estimated from the relative areas A_{shoulder} and A_{peak} of the component diffraction lines using:

$$f_t = (A_{\text{shoulder}}) / (A_{\text{shoulder}} + A_{\text{peak}}). \quad (4)$$

1. DESPER, C.R., and QUARTIERI, T. F. *A System for Programming Angles, Scalar, and Timer by Internal Counting*. Army Materials and Mechanics Research Center, AMMRC TR 72-17, June 1972.
2. WILCHINSKY, Z. W. *X-Ray Diffractometry of Polymers by a Transmission Method*. Adv. X-Ray Anal., v. 8, 1965, p. 151.
3. DESPER, C. R. *Computer Programs for Reduction of X-Ray Diffraction Data for Oriented Polycrystalline Specimens*. Army Materials and Mechanics Research Center, AMMRC TR 72-34, November 1972.
4. GOPALON, M. R., and MANDELKERN, L. *Degree of Crystallinity of Linear Polyethylene from Wide-Angle X-Ray Diffraction*. J. Polym. Science, Polymer Letters, v. 5, 1967, p. 925.
5. CULLITY, B. D. *Elements of X-Ray Diffraction*. Addison-Wesley, Reading, Massachusetts, 1956, p. 466.

The residual stress σ of the material under tension is then obtained using Hooke's Law

$$\sigma = \epsilon E \quad (5)$$

in conjunction with the modulus values of Sakurada,⁶ $E = 4.3 \times 10^4$ kg/cm² and 3.2×10^4 kg/cm² for the 110 and 200 planes, respectively.

X-ray fluorescence was used to detect elements present in minor amounts. A Finnigan QM-900 series instrument incorporating an energy-dispersive detector interfaced to a minicomputer was used. The X-ray tube was used under 16 kV and 1.2 mA excitation. The sample chamber was evacuated and the counting time was 300 seconds. To calibrate the sulfur content, a polyethylene powder (Allied Chemical UHMW grade) was mixed with 0.1% by weight of Santonox R, the specified antioxidant [chemical name 4,4'-thiobis (2-tert-butyl-5-methylphenol)], and molded at 180°C into a flat sheet approximately 1 mm thick to give a standard sample. A blank sample, omitting the Santonox R, was also prepared. Since Santonox R contains 9.82% sulfur, the difference in sulfur content of the two samples is 0.00982%. This figure is used with the sulfur line intensity difference to establish the calibration.

Infrared absorption data were obtained using a Digilab FTS-10M Fourier Transform Scanning Infrared (FTSIR) instrument by attenuated total reflectance.

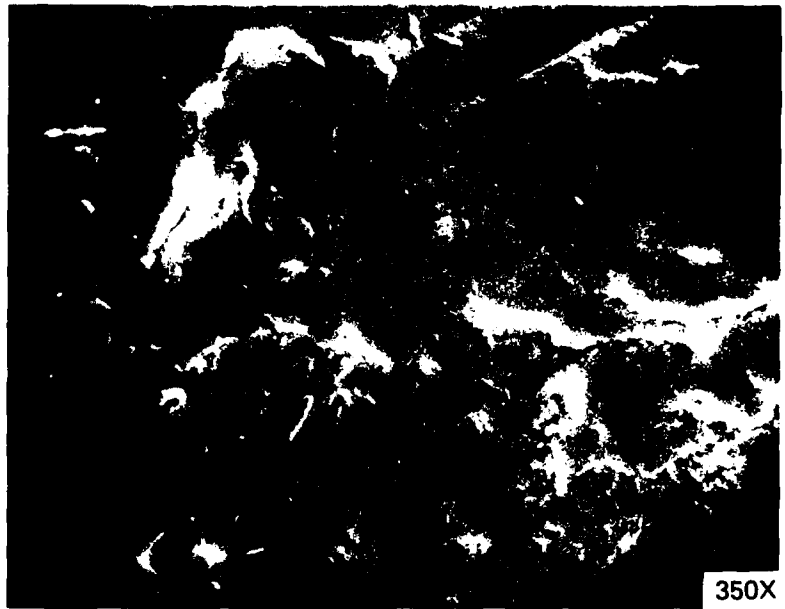
Results

Preliminary Inspection and Microscopic Examination: Examination of the OLD and NEW flat sheet specimens revealed that each sheet has a dull side and a glossy side. These visual differences are confirmed by examination under the scanning electron microscope (SEM). In Figure 1, the smooth side is shown to be largely featureless magnified 350X, except for occasional irregularities which are probably of mechanical origin. On the dull side of the same sheet, these irregularities are more pronounced, but more importantly, spherical structures of about 12 microns diameter fill the field of view. These objects are most likely the well-known spherulites characteristic of polyethylene. Their size is indicative of formation under a slow cooling process. The glossy side was probably quenched by contact with a liquid or a highly-polished chilled metal roller, while the dull side was cooled down from the melt by contact with air.

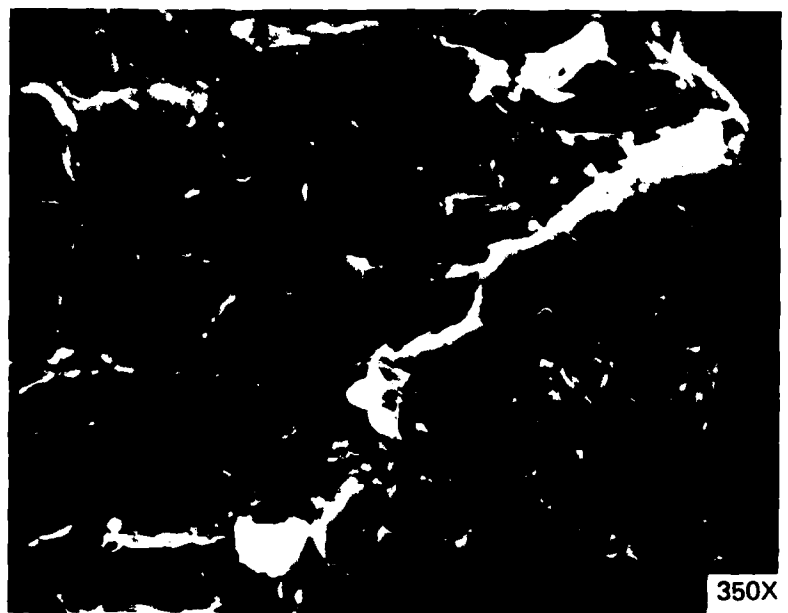
Figure 2 shows a series of SEM photographs of the interior sidewall of an exposed container, taken at various magnifications. At low magnification, structural features in the 25-75 micron size range fill the field, but these appear to be elongated in one direction. These structures are probably spherulites formed and deformed under conditions of flow. The fact that the spherulite size is larger in the extruded tube than in the sheet material indicates crystal growth at a higher temperature, consistent with the slow cooling rates to be expected at the center of an extruded pipe.

In addition, scattered objects one micron in size appear less on the exposed sidewall interior surface, such as the object at the center of Figure 2d. Judging from the texture on the surface of these particles, they are polymeric material. They could be remnants of small spherulites which have undergone chemical attack and are loosely attached to the surface.

6. SAKURADA, I., ITO, T., and NAKAMAE, K. *Elastic Moduli of the Crystal Lattices of Polymers*. J. Polym. Sci., Part C, v. 15, 1966, p. 75.

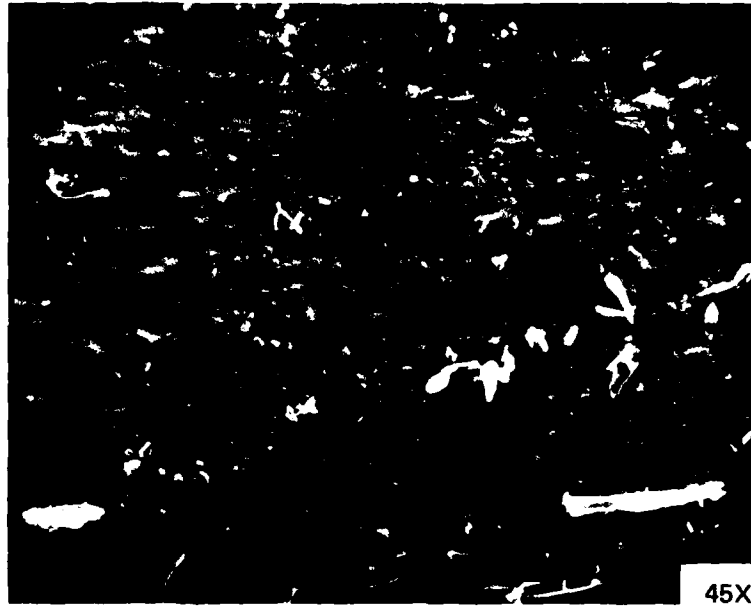


(a)

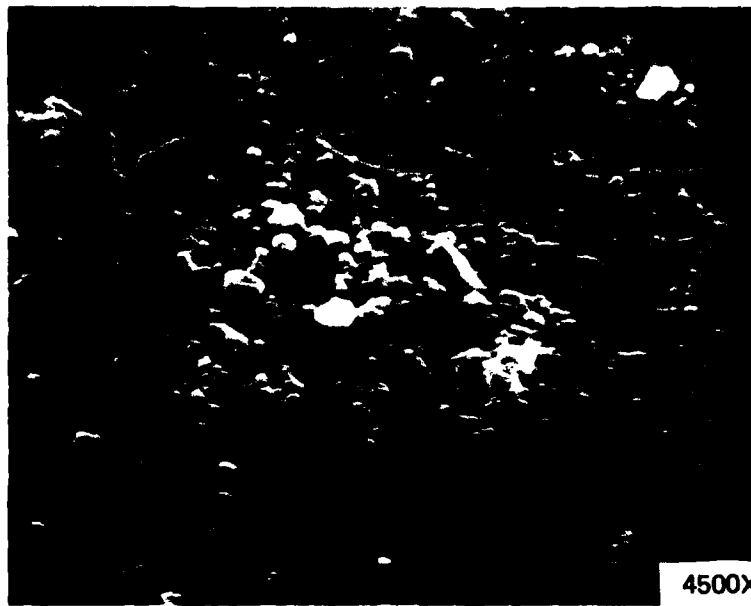


(b)

Figure 1. SEM photographs of NEW - 6-mm flat sheet specimens showing (a) glossy side and (b) dull side.

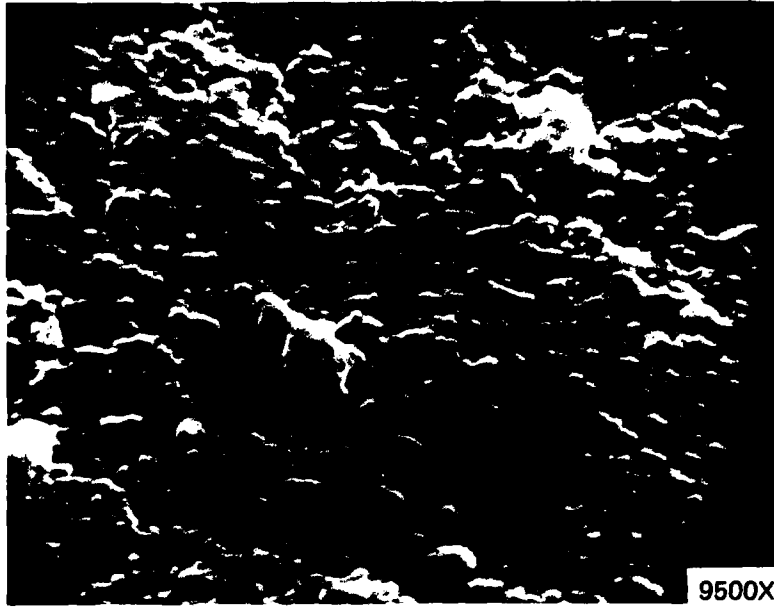


(a)

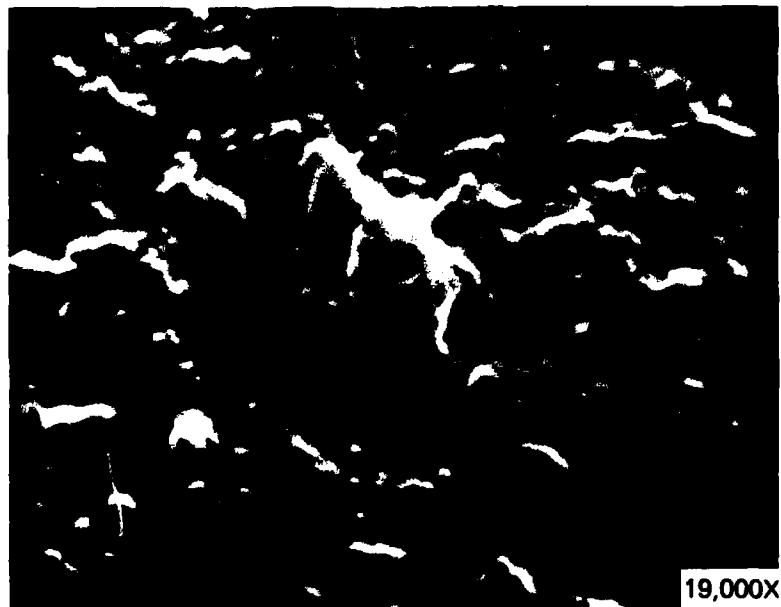


(b)

Figure 2. SEM photographs of interior surface of DF-EXPOSED sidewall container no. 318.



(c)



(d)

Figure 2(cont). SEM photographs of interior surface of DF-EXPOSED sidewall container no. 318.

During the course of sample preparation, a large internal stress became evident in the exposed sidewall material. The burst plates and plug ends were first removed by circumferential cuts on a lathe at a position about 1/8 inch inside the joint. The sidewalls were then split open by two longitudinal cuts. After this was done, it was found that the sidewall pieces would no longer mate mechanically with the end pieces from which they were cut; they had curled to a shorter radius of curvature. The new radius of curvature was measured by placing a half-cylinder of sidewall on circular graph paper and matching its interior and exterior surfaces to semicircles on the paper. The original radius of curvature was measured by calipering the end pieces.

The sidewall dimensions obtained are listed in Table 1 and compared with specification values from MIL-P-51433(EA). The sidewall I.D. is reduced approximately 8% when the internal stress is relieved by splitting the cylinder. The original I.D. is slightly larger at the plug end than at the burst plate, which is noticeably dished inward. However, the sidewall I.D. is lower than specification limits of 105.1 to 109.7 mm, inferred from the O.D. and wall thickness specification, at both ends of the container. This is probably the result of creep occurring after the pipe was extruded, either before canister fabrication or during storage.

Table 1. SIDEWALL DIMENSIONS,
EXPOSED CONTAINER NO. 318

	(mm)	(in.)
I.D. of Cut Sidewall	93.8	3.69
O.D. of Cut Sidewall	109.4	4.31
Sidewall I.D. From Burst Plate	101.6	4.00
Sidewall I.D. From End Plug	102.6	4.04
Sidewall O.D. From MIL-P-51433(EA)	120.1	4.73
Tolerance of O.D.	+0 -1.0	0 -0.040
Sidewall I.D. From MIL-P-51433(EA)	107.4	4.23
Tolerance Of I.D.	+1.3 -2.3	+0.050 -0.090

The physical appearance of the EXPOSED container surfaces is also noteworthy. As seen in Figure 3, the interior sidewall has darkened to a gray-brown color. The burst plate and plug ends are also discolored on the interior surface, but not nearly as much as the sidewall. The exterior surfaces are not discolored. Interestingly, a very faint chord line could be seen on the burst plate. Below this chord line (about 10 mm from the sidewall) the burst plate is discolored, but not above it. This suggests that the container was, at one time, stored on its side and that it was about 90% filled with liquid.

Gel Permeation Chromatography: Figure 4 shows a chromatogram typical of all the polymer solutions studied. The apparent molecular weight values are listed in Table 2. If the samples were known to be strictly linear, these would be true molecular weights. However, the data must be qualified by the term "apparent" until the possible effects of long-chain branching are examined. Short-chain branching (the ethyl side groups) could have a lesser effect on the calibration.

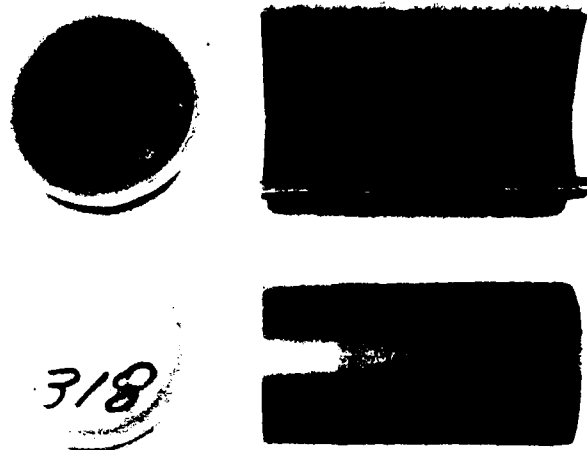


Figure 3. EXPOSED container no. 318. Inner surfaces of end plug and sidewall at top, outer surfaces of burst plate and sidewall at bottom.



Figure 4. Gel permeation chromatogram of ethylene-butene copolymer.

Table 2. SUMMARY OF APPARENT MOLECULAR WEIGHT DATA
AVERAGE VALUES AND STANDARD DEVIATIONS

Sample	M_n	M_w	M_z	M_w/M_n
OLD - 1.5 mm	29,000 (5.8%)	161,700 (5.8%)	423,100 (7.7%)	5.54 (12%)
NEW - 1.5 mm	20,000 (4.3%)	160,000 (1.8%)	430,000 (2.7%)	8.00 (6%)
EXPOSED - 1.5 mm				
Burst Plate No. 317*	24,300 (15.1%)	163,400 (2.4%)	431,800 (1.7%)	6.59 (18%)
Burst Plate No. 317†	23,800 (5.7%)	156,300 (1.3%)	407,700 (2.4%)	6.57 (8%)
OLD - 6 mm				
Dull Side	30,000 (6.5%)	165,000 (1.7%)	410,000 (2.6%)	5.50 (8%)
Glossy Side	30,700 (8.3%)	171,000 (2.5%)	431,000 (3.1%)	5.57 (11%)
NEW - 6 mm				
Dull Side	24,700 (5.8%)	163,000 (0.6%)	419,000 (0.9%)	6.60 (6%)
Glossy Side	23,800 (11.7%)	157,000 (1.9%)	398,000 (3.1%)	6.60 (14%)
EXPOSED - 6 mm				
Sidewall No. 317‡	27,300 (14.4%)	167,400 (1.9%)	435,400 (1.8%)	6.13 (16%)
Sidewall No. 318†	23,900 (19.9%)	159,200 (1.4%)	415,500 (1.6%)	6.66 (21%)
Cap End No. 318*	23,900 (7.2%)	158,800 (1.3%)	409,000 (1.6%)	6.63 (8%)
Cap End No. 318†	23,400 (9.3%)	158,300 (2.2%)	402,300 (4.2%)	6.76 (12%)

Each value is the average of five determinations from a single sample solution.
Standard deviations are in parentheses.

*Sample taken from interior surface

†Sample taken from exterior surface

‡Interior surface samples from exposed sidewalls proved to be insoluble in TCB at 135°C.

Several significant features are evident in the GPC data:

1. The flat-top shape of the polymer molecular weight distribution is quite unusual. This might indicate long-chain branching, but this must be carefully checked against other absolute measures of molecular weight.
2. The molecular weight distribution is quite broad for polyethylene.
3. Very high molecular weight species (about 10^6) are present.
4. There is no significant low molecular weight tail in the distribution.
5. No additives (such as antioxidant) were detected by this method. The sharp peak is attributed to dissolved air; additives would be expected to drive the refractive index detector in the opposite direction.
6. There are significant differences in the number average molecular weight (M_n) values when the OLD samples are compared with the NEW samples. The M_n values

for the OLD samples are consistently in the 30,000 range, while the values for the NEW samples are in the range of 20,000-25,000. The weight-average (M_w) and z-average molecular weights (M_z) are largely unchanged throughout the series.

7. The EXPOSED samples have not undergone any major change in molecular weight characteristics, either on the interior or exterior surfaces. One notable exception is the interior of the sidewall, which has discolored to a grey-brown color, proving to be insoluble in TCB at 135°C. This is indicative of chemical crosslinking. However, the cap end and burst plate of the same containers yielded interior specimens which gave normal solubility behavior and molecular weight data, even though these components had also been in contact with DF liquid or vapor.

8. The consistency of the method is confirmed by examining data for specimens taken from opposite sides of the same samples. The process by which the sheets are manufactured gives the sheets a rough side and a smooth (glossy) side. Referring to Table 2, virtually identical results are obtained from the two sides of a given sample.

Mechanical Properties: The tension test results and the sonic modulus data are given in Tables 3 and 4, respectively. The yield stress values are similar to those observed by Buckley.⁷ There is very little anisotropy in the yield stress data. Ratios of values for machine and transverse direction are close to unity; the differences being, in most instances, slightly higher than the error in the ratio. On the whole, the yield stress data are essentially isotropic.

Table 3. SUMMARY OF TENSILE TEST RESULTS
AVERAGE VALUES AND STANDARD DEVIATIONS

Sample	Yield Stress (psi)		Ratio
	Machine Direction	Transverse Direction	
OLD - 1.5 mm	3159 (1.1%)	3076 (0.8%)	1.03 (1.9%)
NEW - 1.5 mm	3245 (1.4%)	3113 (0.9%)	1.04 (2.3%)
EXPOSED - 1.5 mm Burst Plate No. 317	2960 (0.7%)	N/A	N/A
OLD - 6 mm	3095 (0.9%)	3137 (1.9%)	0.99 (2.8%)
NEW - 6 mm	3347 (0.9%)	3204 (1.9%)	1.05 (2.8%)
EXPOSED - 6 mm Sidewall No. 317	2809 (1.6%)	N/A	N/A
Sidewall No. 318	2960 (0.7%)	N/A	N/A

All values are the averages of five tensile tests. Standard deviations are in parentheses.

For the exposed samples, curvature precluded measurement of yield stress in the transverse direction.

7. CRIST, B. Final Report on Contract DAAA-15-76-C-0077, Northeastern University, Evanston, Illinois, October 1976.

Table 4. SONIC MODULUS DATA

Sample	Modulus at 10 KHz (psi)		Ratio
	Machine Direction	Transverse Direction	
OLD - 1.5 mm	225,000 233,000	278,000 305,000	
Average	229,000	291,500	0.79
NEW - 1.5 mm	223,000 232,000	244,000 274,000	
Average	227,500	259,000	0.88
NEW - 6 mm	252,000 251,000	248,000 265,000	
Average	251,500	256,500	0.98
EXPOSED - 6 mm			
Sidewall No. 317			
Interior	220,000	N/A*	N/A
Exterior	212,000	N/A	N/A
Sidewall No. 318			
Interior	223,000	N/A	N/A
Exterior	206,000	N/A	N/A
Average	215,000		

Note: Samples of sufficient length for this test were not available for OLD - 6 mm and EXPOSED - 1.5 mm.

*For the exposed canisters, curvature precluded measurement of modulus in the transverse direction. Also, burst plate and end cap dimensions are too small to permit sonic modulus measurements.

To look for a difference between the OLD and NEW samples, the grand average yield stress of the former (3117 ± 51 psi) is compared to the grand average yield stress of the latter (3229 ± 96 psi). The 3.5% difference in the two values is not significant considering the error bounds.

The EXPOSED samples give yield stress values in the range of 2800-3000 psi, somewhat below the values for the OLD and NEW materials. However, the values are still well above the specification of 2400 psi [MIL-P-51432(EA)] and the reduction is considered to be of no importance.

The sonic modulus data in Table 4 shows values in the range of 200,000-300,000 psi, consistent with the value of 240,000 psi reported by Charch and Moseley⁸ for unoriented high density polyethylene. The anisotropy was significant for the 1.5-mm samples; modulus ratios were 0.79 and 0.88 for the OLD and NEW samples, respectively. The NEW - 6-mm sample was essentially isotropic at a ratio of 0.98. Modulus values for the EXPOSED - 6-mm sample were comparable to OLD and NEW - 1.5-mm values. It was not possible to test the OLD - 6-mm sample or the EXPOSED - 1.5-mm sample since the dimensions of the specimens were too small for this technique. For polyethylene at room temperature, sonic modulus is particularly sensitive to amorphous orientation, which is probably responsible for the observed anisotropy of the thin sheets. These results are not in conflict with the essentially isotropic behavior observed in yield stress. Sound propagation involves an infinitesimal deformation of the sample, while

8. CHARCH, W. H., and MOSELE, Jr., W. W. *Structure - Property Relationships in Synthetic Fibers, Part I: Structure as Revealed by Sonic Observations*. *Textile Res.*, v. 7, 1959, p. 525.

yielding is an irreversible process occurring in these samples at 10%-12% strain. Factors which cause significant differences in the former experiment could have no effect in the latter.

X-Ray Diffraction: The diffraction pattern of a typical sample is given in Figure 5. Two different exposure times are shown to bring weaker and stronger lines into optimum contrast. The pattern, and those of all the other samples, shows essentially no overall crystalline orientation in these polyethylenes.

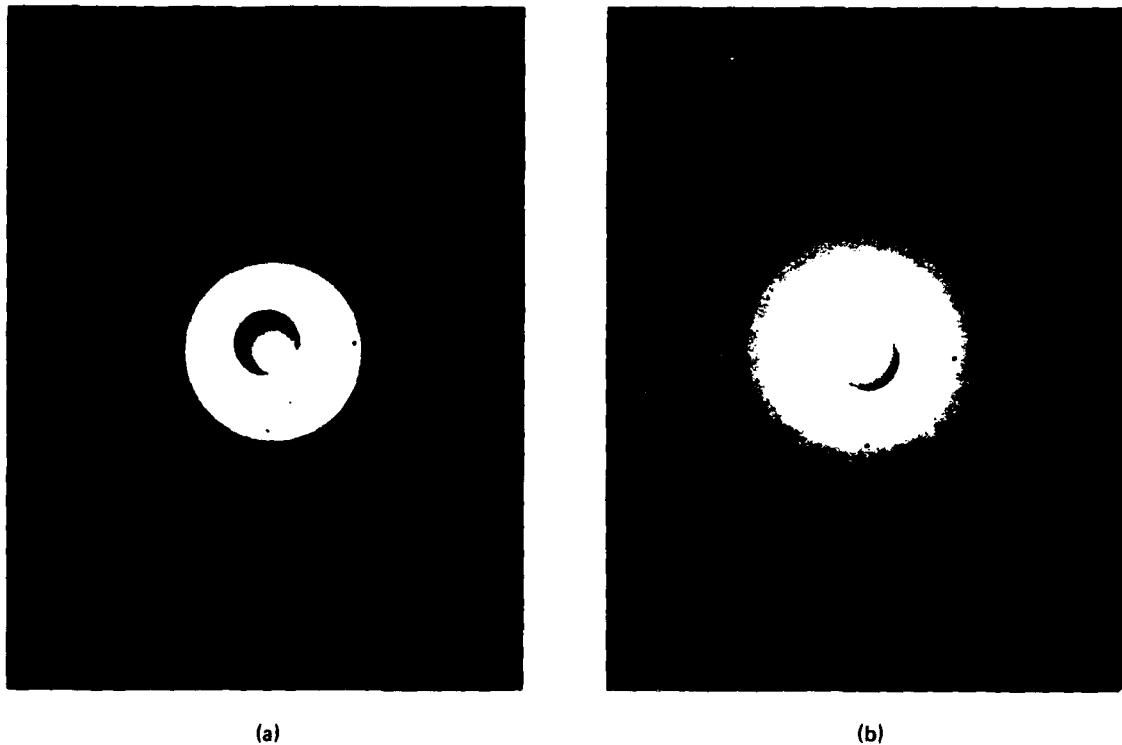


Figure 5. X-ray diffraction pattern of NEW - 1.5-mm sample. Machine direction vertical; (a) 28 minute exposure and (b) 60 minute exposure.

Quantitative X-ray diffraction data were obtained using both the transmission and reflection modes of operation shown in Figure 6. The modes differ in two important ways: the material sampled and the direction of orientation of the crystallites being sampled. The reflection method (Figure 6a) responds primarily to material near the surface for thick specimens, since the signal from the interior material is strongly attenuated by sample absorption. The actual depth of penetration of the X-rays depends upon X-ray wavelength, sample composition, and 2θ value. For the present studies it is estimated that the average depth of penetration is 0.15 mm; a small fraction of the total thickness of the 1.5-mm or 6-mm specimens. The transmission mode (Figure 6b) gives a true average over the thickness of the specimen. However, intensity is greatly weakened by absorption for thick specimens, such as the 6-mm polyethylenes.

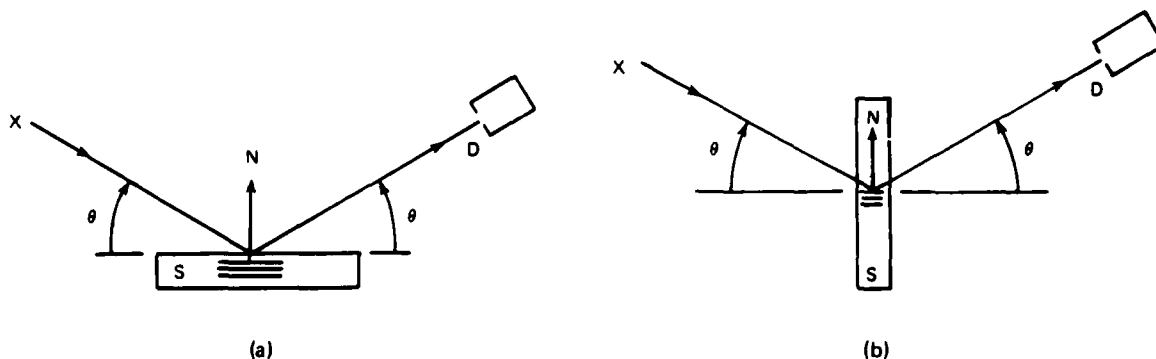


Figure 6. Modes of operation of X-ray diffractometer with (a) the reflection method and (b) the transmission method showing (D) detector; (S) sample; (N) diffracting plane normal; and (θ) diffraction angle.

In addition, the reflection method detects crystallites oriented with their diffraction plane normals parallel to the sheet normal, while the transmission method responds to crystallites with their diffraction plane normals in the plane of the sheet. In the course of this work, a significant difference in the diffraction pattern was observed which is attributed to this difference in direction. Figures 7 and 8 are the diffraction patterns for the same sample (NEW - 6 mm) in reflection and in transmission. The reflection pattern (Figure 7) is resolved mathematically into three components: a broad amorphous peak centered at 20.782° , and the 110 and 200 crystal reflections at 21.304° and 23.698° . Additional shoulders appear on the low angle sides of the two crystal peaks (Figure 8) for the transmission pattern. A satisfactory resolution of the curves requires five component curves: the amorphous peak; two 110 peaks at 21.052° and 21.600° ; and two 200 peaks at 23.336° and 23.978° . The resolution of the split 110 and 200 peaks is shown in Figures 9 and 10.

The appearance of the shoulders indicates residual stress. It occurs in the transmission pattern and not the reflection pattern simply because the stresses are acting in the plane of the sheet and are zero normal to the sheet. Thus, the crystallites, which act as tiny stress gauges, deform solely in the plane of the sheet. The calculated results, shown in Table 5, indicate that the crystallites are strained an average of 2.6% for the six specimens studied. One sample (OLD - 1.5 mm) shows less residual strain (about 2.0%) than the other five, which do not differ significantly in residual strain.

Converting the crystallite residual strains into residual stresses is a problem. The figures given in Table 5 for residual stress use the known crystal modulus values and presume Hookean (linear) behavior. However, Sakurada⁶ does not state the strain range for which his modulus values for polyethylene are valid. Thus, there is no guarantee that the stress-strain curve remains linear up to the 2% to 3% strain levels encountered here. Although the residual strain data reported here is valid, the use of the initial modulus may result in overestimated values of the residual stress.

In this regard, it is notable that the values of residual strain, as measured from the 110 and 200 reflections, are generally in agreement for a given sample, while the 110 data gives higher residual stress values because of the higher modulus value used for the 110 planes. This difference could be an artifact arising from departures from linearity in the stress-strain curves for either the 110 or 200 planes, or both.

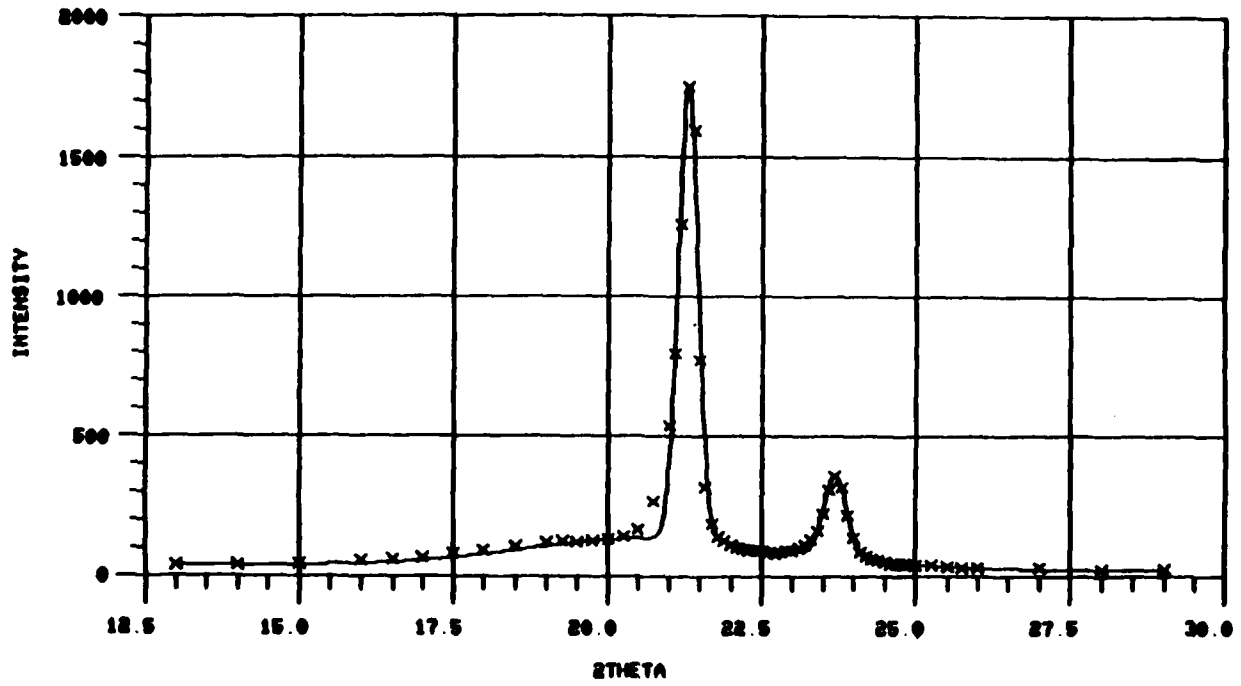


Figure 7. Reflection X-ray diffraction pattern, NEW - 6 mm.

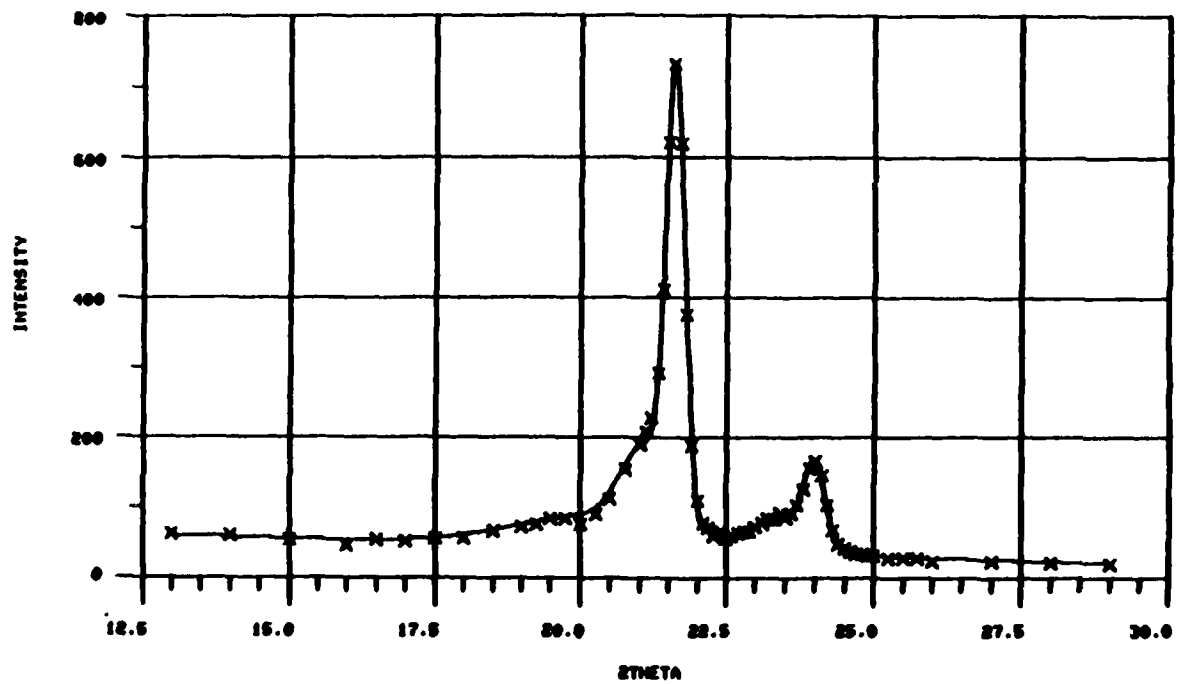


Figure 8. Transmission X-ray diffraction pattern, NEW - 6 mm.

AD UNCLASSIFIED
UNLIMITED DISTRIBUTION
Key Words

Army Materials and Mechanics Research Center,
Watertown, Massachusetts 02172
CHARACTERIZATION AND SELECTION OF POLYMER
MATERIALS FOR BINARY MUNITIONS STORAGE -
C. Richard Desper

Technical Report AMMRC TR 83-45, August 1983, 29 pp - Polyethylene
illius-tables, D/A Project IL162622A554
AMCMS Code 6126225540A11

The purpose of this study was to investigate the materials properties required for storage of DF (methylphosphonic difluoride) over extended periods of time at temperatures as high as 70°C, anticipating more severe environmental requirements. Specimens of nominally 96/4 ethylene/propylene copolymer were examined by SEM, GPC, FTIR, X-ray diffraction, and tensile testing. Specimens fabricated into containers and exposed to DF for eight years were compared to control samples of the same vintage and to newly processed polymer sheets of the same resin type. The molecular weight distributions were broad, with M_w values of 160,000 to 170,000 and M_n values of 24,000 to 30,000. These values were unaffected by exposure to DF with the exception of the interior sidewall, which had been in contact with liquid DF and showed a narrow surface layer of discolored cross-linked material. X-ray diffraction showed the expected 60% crystallinity, but also revealed a pattern of residual stress. However, no loss in mechanical properties was observed. The environmental stress cracking process is the major factor contributing to premature failure in DF containers, with polymer oxidation playing only a secondary role. Materials and processing factors affecting performance are discussed. Further work continues in this area.

AD UNCLASSIFIED
UNLIMITED DISTRIBUTION
Key Words

Army Materials and Mechanics Research Center,
Watertown, Massachusetts 02172
CHARACTERIZATION AND SELECTION OF POLYMER
MATERIALS FOR BINARY MUNITIONS STORAGE -
C. Richard Desper

Technical Report AMMRC TR 83-45, August 1983, 29 pp - Polyethylene
illius-tables, D/A Project IL162622A554
AMCMS Code 6126225540A11

The purpose of this study was to investigate the materials properties required for storage of DF (methylphosphonic difluoride) over extended periods of time at temperatures as high as 70°C, anticipating more severe environmental requirements. Specimens of nominally 96/4 ethylene/propylene copolymer were examined by SEM, GPC, FTIR, X-ray diffraction, and tensile testing. Specimens fabricated into containers and exposed to DF for eight years were compared to control samples of the same vintage and to newly processed polymer sheets of the same resin type. The molecular weight distributions were broad, with M_w values of 160,000 to 170,000 and M_n values of 24,000 to 30,000. These values were unaffected by exposure to DF with the exception of the interior sidewall, which had been in contact with liquid DF and showed a narrow surface layer of discolored cross-linked material. X-ray diffraction showed the expected 60% crystallinity, but also revealed a pattern of residual stress. However, no loss in mechanical properties was observed. The environmental stress cracking process is the major factor contributing to premature failure in DF containers, with polymer oxidation playing only a secondary role. Materials and processing factors affecting performance are discussed. Further work continues in this area.

AD UNCLASSIFIED
UNLIMITED DISTRIBUTION
Key Words

Army Materials and Mechanics Research Center,
Watertown, Massachusetts 02172
CHARACTERIZATION AND SELECTION OF POLYMER
MATERIALS FOR BINARY MUNITIONS STORAGE -
C. Richard Desper

Technical Report AMMRC TR 83-45, August 1983, 29 pp - Polyethylene
illius-tables, D/A Project IL162622A554
AMCMS Code 6126225540A11

The purpose of this study was to investigate the materials properties required for storage of DF (methylphosphonic difluoride) over extended periods of time at temperatures as high as 70°C, anticipating more severe environmental requirements. Specimens of nominally 96/4 ethylene/propylene copolymer were examined by SEM, GPC, FTIR, X-ray diffraction, and tensile testing. Specimens fabricated into containers and exposed to DF for eight years were compared to control samples of the same vintage and to newly processed polymer sheets of the same resin type. The molecular weight distributions were broad, with M_w values of 160,000 to 170,000 and M_n values of 24,000 to 30,000. These values were unaffected by exposure to DF with the exception of the interior sidewall, which had been in contact with liquid DF and showed a narrow surface layer of discolored cross-linked material. X-ray diffraction showed the expected 60% crystallinity, but also revealed a pattern of residual stress. However, no loss in mechanical properties was observed. The environmental stress cracking process is the major factor contributing to premature failure in DF containers, with polymer oxidation playing only a secondary role. Materials and processing factors affecting performance are discussed. Further work continues in this area.

AD UNCLASSIFIED
UNLIMITED DISTRIBUTION
Key Words

Army Materials and Mechanics Research Center,
Watertown, Massachusetts 02172
CHARACTERIZATION AND SELECTION OF POLYMER
MATERIALS FOR BINARY MUNITIONS STORAGE -
C. Richard Desper

Technical Report AMMRC TR 83-45, August 1983, 29 pp - Polyethylene
illius-tables, D/A Project IL162622A554
AMCMS Code 6126225540A11

The purpose of this study was to investigate the materials properties required for storage of DF (methylphosphonic difluoride) over extended periods of time at temperatures as high as 70°C, anticipating more severe environmental requirements. Specimens of nominally 96/4 ethylene/propylene copolymer were examined by SEM, GPC, FTIR, X-ray diffraction, and tensile testing. Specimens fabricated into containers and exposed to DF for eight years were compared to control samples of the same vintage and to newly processed polymer sheets of the same resin type. The molecular weight distributions were broad, with M_w values of 160,000 to 170,000 and M_n values of 24,000 to 30,000. These values were unaffected by exposure to DF with the exception of the interior sidewall, which had been in contact with liquid DF and showed a narrow surface layer of discolored cross-linked material. X-ray diffraction showed the expected 60% crystallinity, but also revealed a pattern of residual stress. However, no loss in mechanical properties was observed. The environmental stress cracking process is the major factor contributing to premature failure in DF containers, with polymer oxidation playing only a secondary role. Materials and processing factors affecting performance are discussed. Further work continues in this area.

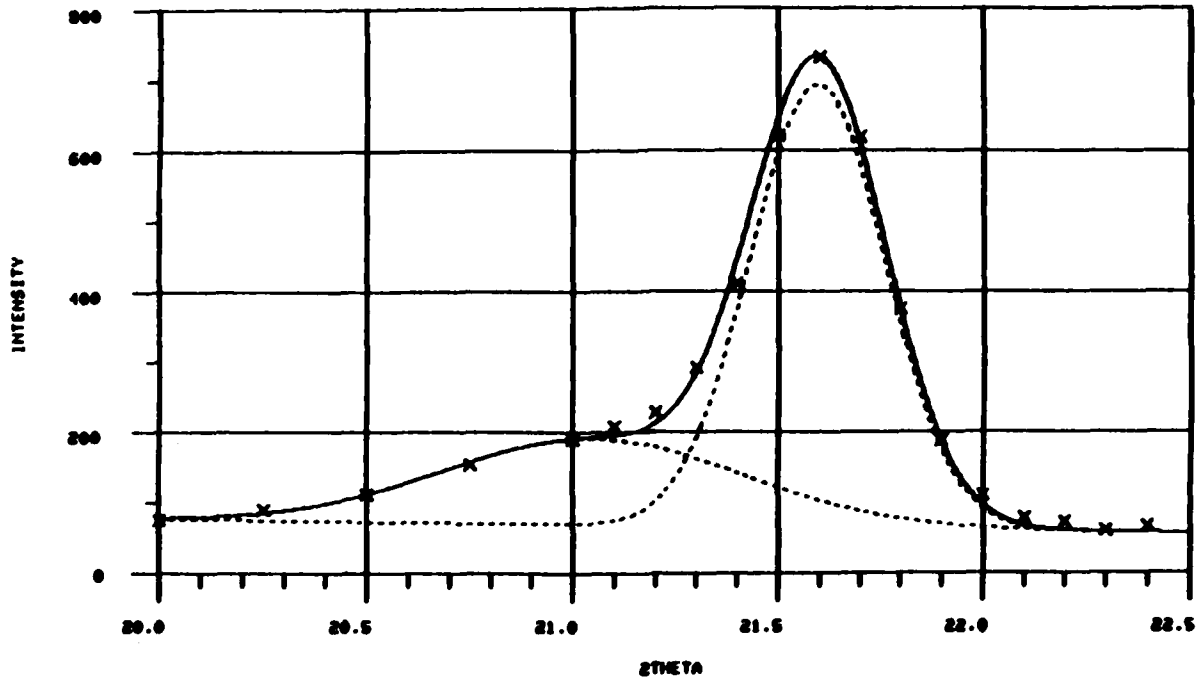


Figure 9. 110 plane peak and shoulder resolution, NEW - 6 mm, transmission mode.

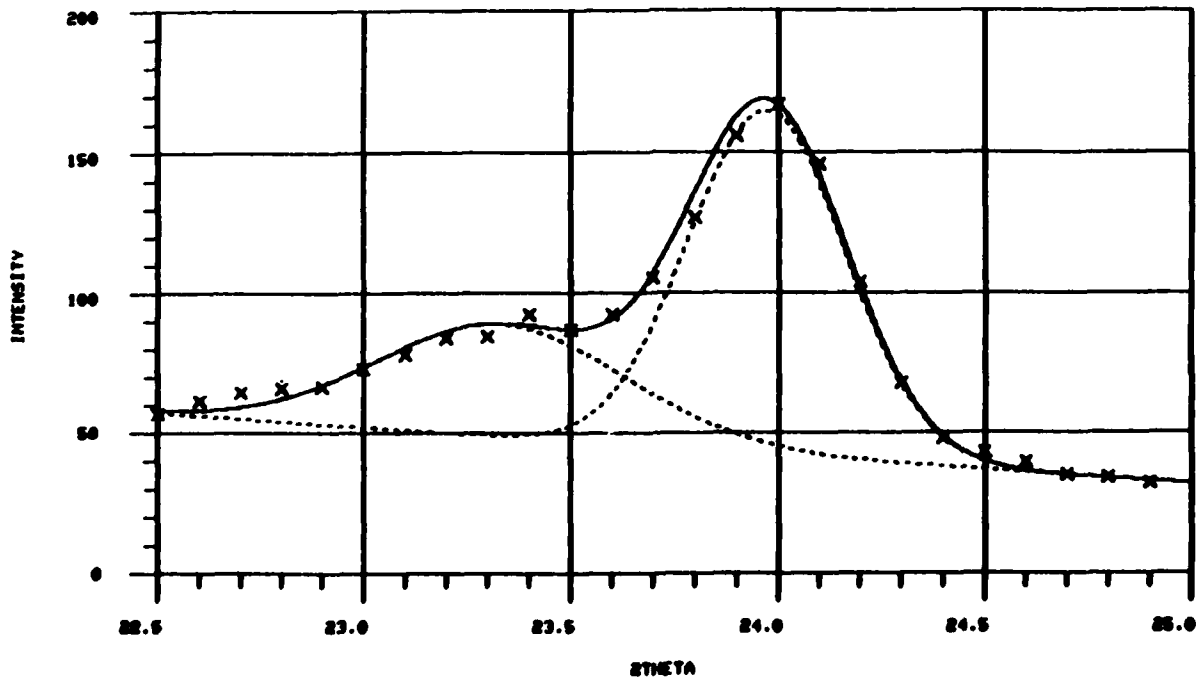


Figure 10. 200 plane peak and shoulder resolution, NEW - 6 mm, transmission mode.

Table 5. RESIDUAL STRAIN DATA FROM X-RAY DIFFRACTION
TRANSMISSION METHOD USED

Sample	Results from 110 Plane			Results from 200 Plane		
	ϵ	τ , psi	f_t	ϵ	τ	f_t
OLD - 1.5 mm	0.019	12,000	0.30	0.022	10,000	0.18
OLD - 6 mm	0.030	18,000	0.24	0.031	14,000	0.25
NEW - 1.5 mm	0.029	18,000	0.15	0.024	11,000	0.19
NEW - 6 mm	0.025	15,000	0.27	0.026	12,000	0.28
EXPOSED - 1.5 mm Burst Plate No. 317	0.025	15,000	0.21	0.024	11,000	0.15
EXPOSED - 6 mm Sidewall No. 317	0.027	16,000	0.44	0.026	12,000	0.29
Average	0.026	16,000	0.27	0.026	12,000	0.22

Based on crystal modulus values of 610,000 psi (110 direction),
and 454,000 psi (200 direction).

The crystallinity values determined by X-ray diffraction, as determined in both reflection and transmission modes, are listed in Table 6. The reflection method gives an average value of 0.62 for X_c with a standard deviation of 0.03, which compares favorably with the uncertainty value of 0.05 reported by Gopalan and Mandelkern⁴ for this determination. The transmission method gives the same average value of 0.62 with more scatter, probably due to the greater uncertainty in resolving the more complicated crystal peaks in the presence of residual stress effects. Within experimental error, the crystallinity is identical for all six specimens, and the reflection values are preferred.

Table 6. CRYSTALLINITY VALUES FROM X-RAY DIFFRACTION

Sample	Crystallinity, X_c	
	Reflection Mode	Transmission Mode
OLD - 1.5 mm	0.60†	0.56
OLD - 6 mm	0.67†	0.70
NEW - 1.5 mm	0.63†	0.56
NEW - 6 mm	0.59†	0.71
EXPOSED - 1.5 mm	0.62‡	0.56
EXPOSED - 6 mm*	0.58‡	0.64
Average	0.62	0.62
Standard Deviation	0.03	0.07

*Sidewall
†Glossy side of flat sheet
‡Interior surface of container

The crystallinity values from reflection are particularly important because these values indicate material properties at an average depth of only 0.15 mm or 0.006 inches, and would show the greatest effect of environmental exposure. In all six cases the data was taken on the surface which had either been exposed to DF, or was intended for exposure to DF. It is remarkable that even the interior sidewall of the exposed container, which is greatly discolored (see Figure 3) and has been rendered insoluble by chemical attack, has not significantly changed in crystallinity. (This specimen gives the lowest reflection method of crystallinity, a value of 0.58, but the uncertainty in the data renders this difference inconclusive.) Evidently,

the chemical attack has been confined to the amorphous regions. In this regard the X-ray determination of crystallinity is more reliable than a density determination, since chemical attack may be expected to increase the density of the amorphous regions. Such an increase in density with chemical attack was interpreted as indicative of an increase in crystallinity by Crist,⁷ however, this need not be the case. An oxidative attack which converts a fraction of the amorphous phase methylene (CH₂) groups to carbonyl (C=O) groups, for example, would increase the density while decreasing the weight average crystallinity. The accompanying increase in crystallinity, as determined by infrared absorption, could also be spurious. The infrared method measures the ratio of crystalline to amorphous methylene groups and would be biased toward the crystalline side by preferential attack on the amorphous methylene groups.

The material specification [MIL-P-51431(EA)] requires a density ρ in the range of 0.939 to 0.943 g/cm³, however, density values are not presently available. For the purpose of comparison, however, one may refer to the cross-correlation between X-ray crystallinity by Equation 1 and density in the data of Gopalan and Mandelkern.⁴ Fitting a least-squares straight line to that data, one obtains:

$$(1/\rho) = 1.170 - 0.171 X_C \quad (6)$$

with a correlation coefficient of 0.997. Using this correlation, the specification density range of 0.939 to 0.943 corresponds to a crystallinity range of 0.61 to 0.64 which brackets the mean X-ray value of 0.62 from Table 6. Consequently, there is every reason to believe that the materials meet the density specification.

X-Ray Fluorescence: Table 7 summarizes the elements detected (P and S) by X-ray fluorescence. There were no detectable amounts of Si, Cl, or Fe, and the method is not sensitive to F. Because of the low penetrating power of the characteristic X-ray lines of P and S, the data represents material composition quite close to the sample surface.

Table 7. X-RAY FLUORESCENCE RESULTS

Sample	Net Counts		S Content, %	S Reported as Santonox R, %
	P	S		
Molded PE Standard	984	2382	0.013	0.130
Molded PE Blank	1061	532	0.003	0.030
OLD - 6 mm	923	1073	0.005	0.05
NEW - 6 mm	671	1531	0.008	0.08
EXPOSED - 6 mm*				
Exterior	1615	1593	0.008	0.08
Interior	9204	7484	0.040	0.4

*Sidewall no. 317

The sulfur content is reported as weight percent Santonox R in Table 7. All of the samples, except one, appear to contain a reasonable amount of antioxidant, but somewhat below the specified 0.1%. However, the data is considered only semi-quantitative at this point since the method is subject to the uncertainty of possible differences between bulk and surface composition. The interior surface of the exposed sidewall is quite high in sulfur content, four times the specification content, while the exterior of the same sidewall is slightly below the specification sulfur content. The high sulfur content on the exposed interior surface could

result from a chemical reaction at the surface, converting Santonox R to a different sulfur-containing compound, followed by migration of additional antioxidant to the surface to replace the depleted Santonox R content. A possible mechanism will be discussed later. However, the possibility that the container picked up sulfur-containing impurities from the DF liquid cannot be ruled out.

Since no phosphorus-containing standard was used, the phosphorus data in Table 7 cannot be placed on an absolute basis. However, comparison of the relative phosphorus contents of the various samples can be instructive. All of the unexposed samples contain appreciable and comparable amounts of phosphorus from an unspecified source. The exposed sidewall shows large amounts of phosphorus; approximately 50% greater than the unexposed samples at the outer surface, and nine times the content of the unexposed samples at the inner surface. Evidently, the phosphorus, in the form of DF, has been slowly diffusing through the sidewall while in storage, resulting in higher phosphorus levels and a concentration gradient. Possibly some phosphorus has been chemically bonded to the polymer; the evidence is inconclusive on this point.

Infrared Absorption: FTSIR data were obtained in the frequency range of 400-4000 cm^{-1} . In addition to the polyethylene bands at 720, 730, 1303, 1352, 1369, 1460, 1470, 2850, and 2920 cm^{-1} , extraneous bands were seen at 1100-1200 cm^{-1} (C-O), 1600 cm^{-1} (O-H), 1744 cm^{-1} (C=O), and 3350-3400 cm^{-1} (O-H). Figures 11 through 17 show the spectra obtained in the range of 1000-1800 cm^{-1} . Although the intensity scales are arbitrary, the absorbance data may be placed on a common basis by reference to the intensities of the strongest polyethylene band at 2920 cm^{-1} . Thus, the relative carbonyl content of the various samples may be compared by using the ratio (A_{1744}/A_{2920}) as shown in Table 8. Of the samples tested, the interior sidewall of the exposed container shows, by far, the greatest carbonyl content. The only pattern evident for the remaining samples is the low carbonyl content of the 1.5-mm samples compared to the 6-mm samples. This probably originates in the extrusion processing; as the extrudate emerges from the die, the thinner extrudates cool more quickly and is less susceptible to surface oxidation.

Table 8. COMPARISON OF CARBONYL FTSIR BAND INTENSITIES

Sample	A_{1744}^\dagger	A_{2920}^\dagger	A_{1744}/A_{2920}
OLD - 1.5 mm	0.40	39.0	0.010
OLD - 6 mm	0.42	5.1	0.082
NEW - 1.5 mm	0.57	53.2	0.011
NEW - 6 mm	0.53	18.7	0.028
EXPOSED - 1.5 mm Burst Plate No. 317, Interior	0.66	46.1	0.014
EXPOSED - 6 mm* Exterior	0.24	10.7	0.022
Interior	1.41	8.5	0.17

*Sidewall no. 317

†Arbitrary units

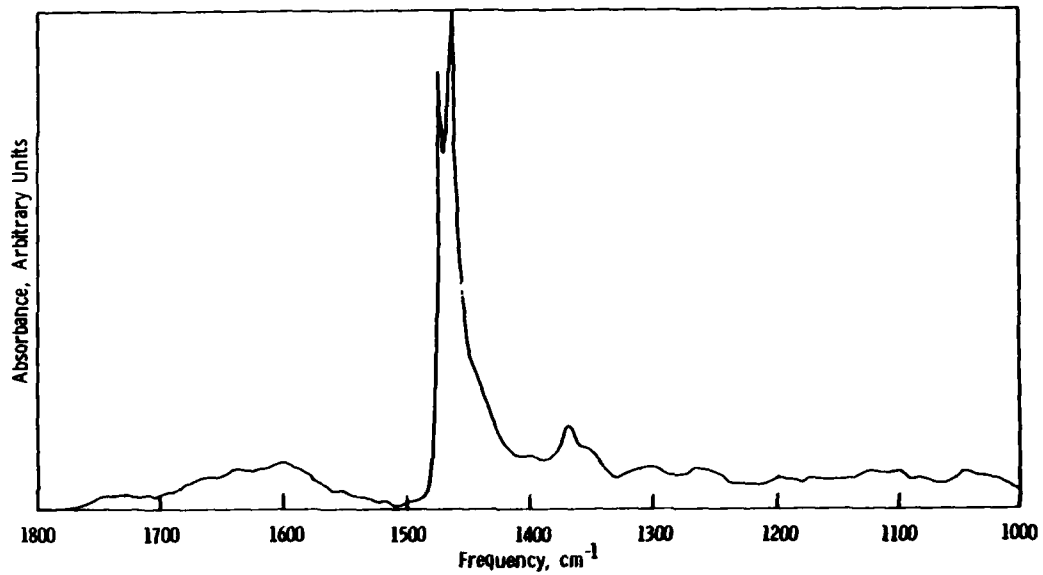


Figure 11. OLD - 1.5 mm (glossy side).

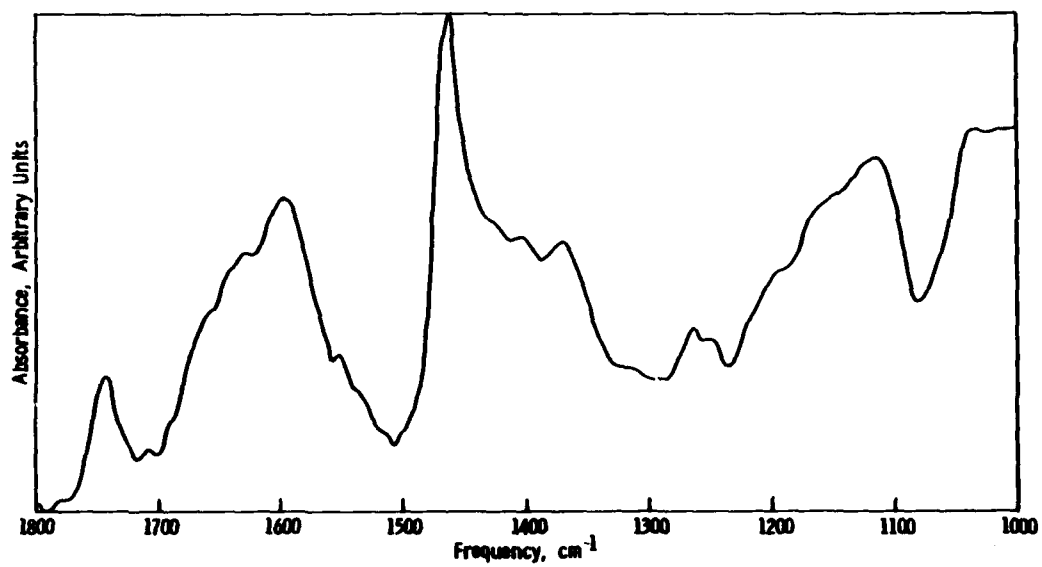


Figure 12. OLD - 6 mm (glossy side).

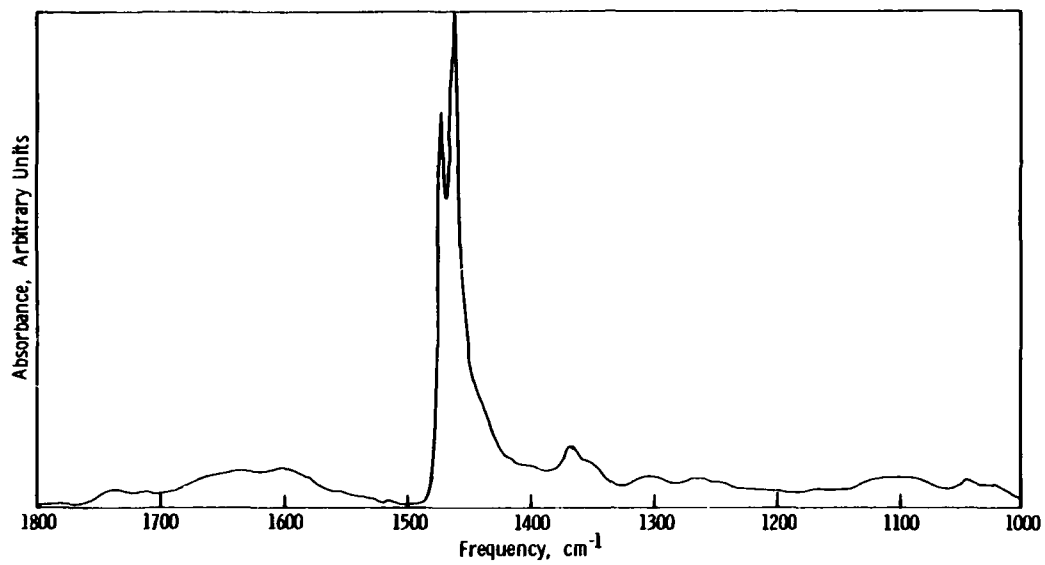


Figure 13. NEW - 1.5 mm (glossy side).

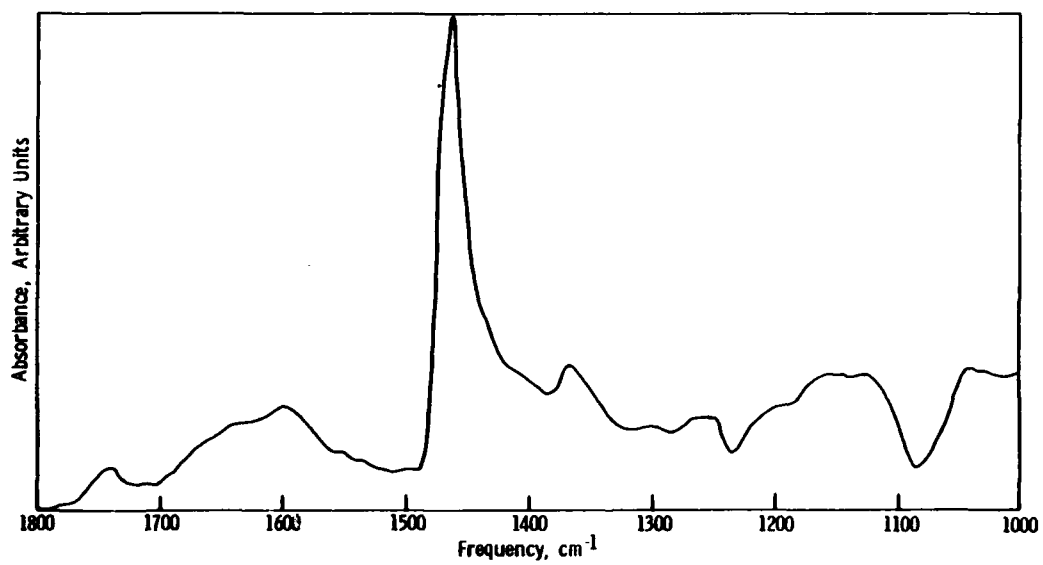


Figure 14. NEW - 6 mm (glossy side).

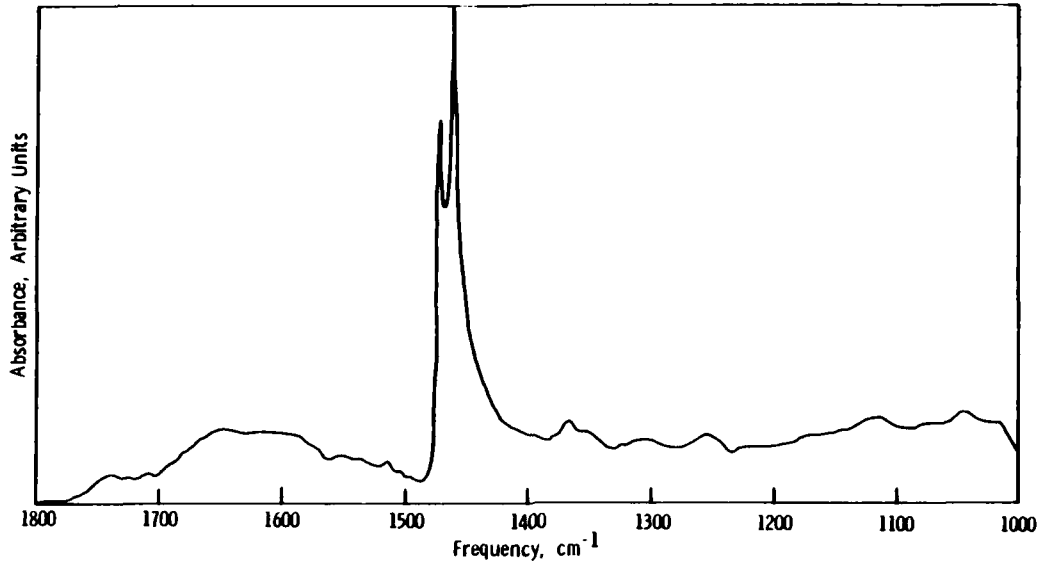


Figure 15. EXPOSED - 1.5 mm (interior).

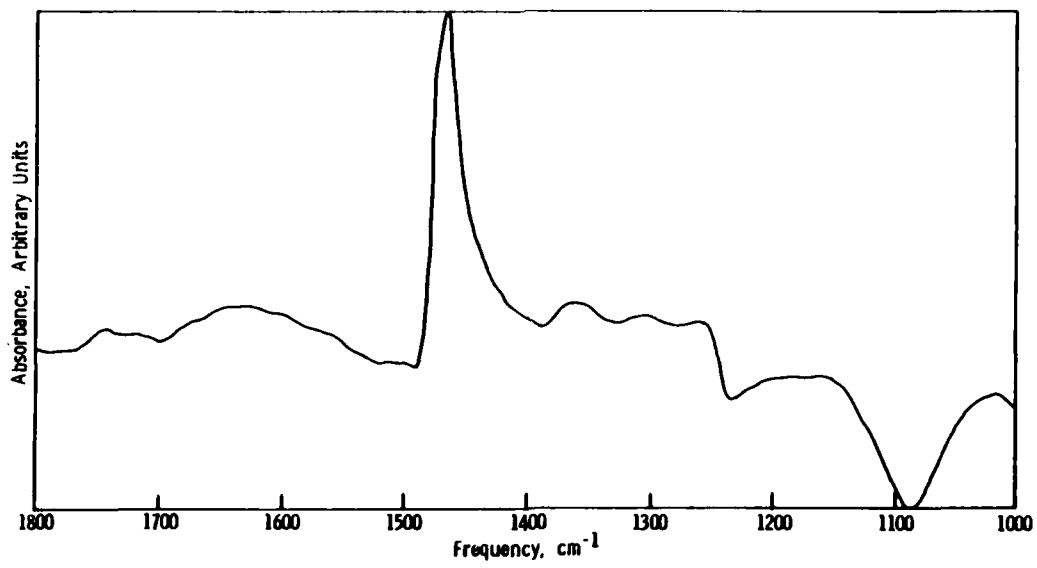


Figure 16. EXPOSED - 6-mm sidewall no. 317 (exterior).

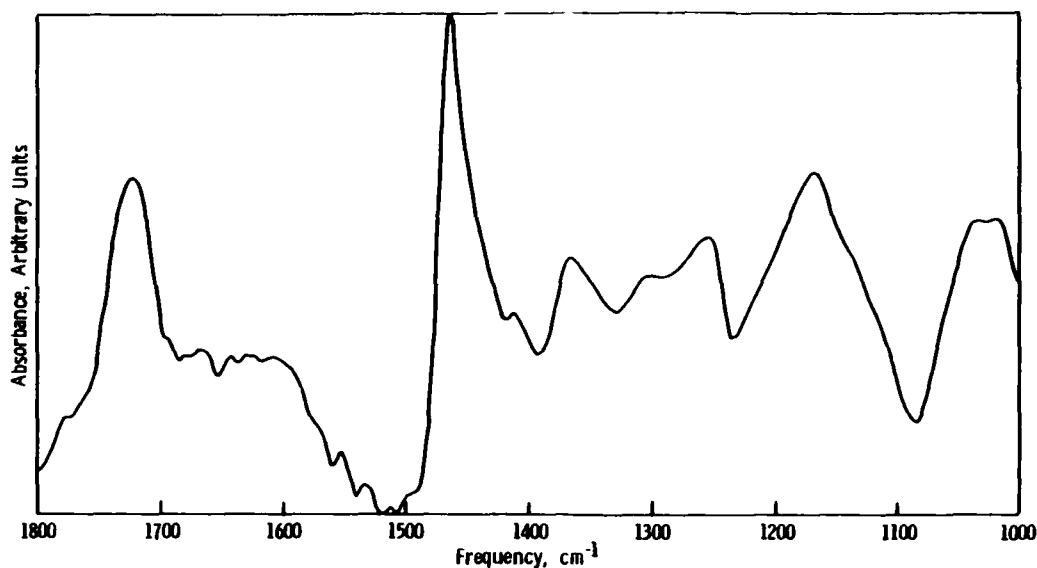


Figure 17. EXPOSED - 6-mm sidewall no. 317 (interior).

The exterior surface of the exposed 6-mm sidewall shows far less carbonyl content than the interior of the same sidewall by a factor of about eight. As shown in Figure 3, the high carbonyl content of the interior results from the same oxidative attack which causes discoloration. Interestingly, the burst plate interior of the same container, which shows only faint discoloration, is quite low in carbonyl content.

The methyl band at 1378 cm^{-1} , which appears in the Crist report⁷ and in the material specification MIL-P-51431(EA), is not observed. This band is overshadowed by the strong band at 1369 cm^{-1} and was observed as a separate peak, rather than a shoulder, only by using a wedge of presumably linear polyethylene in the reference beam to cancel out the 1369 cm^{-1} line. This was not done in the present work since the FTSIR is a single-beam instrument. The determination of butene content, or short-chain branching, by use of the 1378 cm^{-1} band is not a simple procedure, and a better method is desired.

DISCUSSION

The Crist report⁷ emphasizes the role of oxidative attack in the mechanism of failure, while minimizing the importance of environmental stress cracking. However, the field of environmental stress cracking has seen an explosion of activity since 1976, resulting in over forty publications on polyethylene alone. In light of this knowledge, the author believes that the relative importance of these two factors should be reversed. Oxidative attack does not explain a prevalent feature of incipient failure in DF containers as first reported by White et al.⁹ which is the phenomenon of blistering. Blistering involves the formation of disk-shaped subsurface voids filled with liquid. The location of these voids below the surface, rather

9. WHITE, S. S., LEEP, D. A., FIELDER, D., and DUNNE, L. P. *The Permeation of the Chemical Components of the Binary G-Munition Through Polyethylenes*. Edgewood Arsenal Technical Report EC-TR-74080, AD-C000378, Aberdeen Proving Ground, Maryland, November 1974.

than at the surface, suggests an association with internal stresses rather than with oxidation. Crist also reports that container failure is associated with high thermal shrinkage ratios and with broader, and sometimes multiple, melting endotherms. Both effects can result from nonuniform internal stresses.

Bubeck¹⁰ describes environmental stress cracking in terms of originally dry microvoids that fill with liquid and grow in size under the driving force of capillary pressure to form crazes and, eventually, cracks. Shanahan and Schultz¹¹ further describe this mechanism in relation to the nature of the liquid and the level of applied stress. Applied stress activates the failure process by reducing the incubation time for crack formation; residual stress may have the same effect. In this instance, the aggressive characteristics of DF liquid, combined with high residual stress, can lead to premature failure. The fact that the disk-like shape of the blisters follows the planar pattern of residual stress suggest very strongly that environmental stress cracking is involved.

In the absence of catastrophic failure brought on by environmental stress cracking, polymer oxidation is largely confined to a thin zone near the surface in contact with the DF liquid. Crist⁷ reports higher levels of oxidation, as indicated by higher density and IR crystallinity, and by increased unsaturation, carbonyl groups, and optical discoloration, in the failed containers. However, this oxidation may be the result of the failure process rather than its cause. As environmental stress cracking proceeds, the crazes and cracks generated in the process constitute a large internal surface accessible to the same oxidative influences as the external polymer surface, so the polymer oxidizes internally as well as externally. In the absence of environmental stress cracking the oxidation would have been small.

Postulating that environmental stress cracking precedes the oxidation process may explain the pattern of oxidation observed in the exposed containers. The polymer processing leaves frozen-in strains in the materials in both the sheet and the tube forms. The sheet material has a three-layer structure, as described by Crist,⁷ with zones of compressed material on the outside surfaces and material under tension in the core. The tubing has a two-layer structure, like a circular bimetallic spring, with a zone of compression on the outside and a zone of tension on the inner surface. Thus, of the surfaces wetted by liquid DF, the interior tubing surface will be under tension, and therefore predisposed to the opening of microcracks, while the sheet surfaces at both ends are not as predisposed, since the surface material there is in compression. In fact, the oxidation which occurs at the interior surface of the tubing results in crosslinking, which holds the material together; this process is self-healing in the present instance.

There are two possible roles of DF liquid in promoting oxidative attack on the polymer: first, the passive role of depleting the antioxidant, and second, a more active role of promoting oxidation through the physical action of DF on the polymer itself. The surface concentration of sulfur does suggest that DF reacts with the antioxidant to render it ineffective, but this is not conclusively shown to be its primary role. On the other hand, if the DF (or an impurity in the DF, such as HF) promotes oxidation itself, it would not be through the usual free radical initiation

10. BUBECK, R. A. *Kinetics of Environmental Stress Cracking in High Density Polyethylene*. *Polymer*, v. 22, 1981, p. 682.

11. SHANAHAN, M. E. R., and SCHULTZ, J. *Environmental Stress Cracking of Polyethylene: Analysis of the Three Zones of Behavior and Determination of Crack-Front Dimensions*. *J. Polym. Sci., Polym. Phys. Ed.*, v. 18, 1980, p. 19.

path. The chemical structure of DF (and HF, for that matter) is notably lacking in homonuclear bonds and is not a likely source of free radicals. In that case, the usual polymer antioxidants would be ineffective, since they are designed to interfere in a free radical chain reaction. Instead, it might be possible to render the polymer surface chemically inert by fluorination of the polyethylene surface to yield a thin coating of poly (tetrafluorethylene). The strong oxidizing power of fluorine must be mitigated to result in surface fluorination rather than destruction of the polymer, however, there are reports of success in achieving surface fluorination of polyethylene items.

The environmental stress cracking failure mechanism is influenced very strongly by the material characteristics of the polyethylene resin, as well as by processing. Molecular weight, crystallinity, and short-chain branching influence the number of intercrystalline links; i.e., the number of polymer segments connecting one crystallite to another. These intercrystalline links are the major obstacle to crack growth and, therefore, the key to resistance to environmental stress cracking. Medium crystallinity is desired rather than high crystallinity, since the latter is associated with the greater crystallite perfection and a higher degree of regular chain folding. (Regular chain folding, in which a crystallizing polymer molecule reaches the crystallite surface, then turns back into the same crystallite, is the antithesis of the desired intercrystalline link. The concept of the intercrystalline link is discussed in a number of basic polymer textbooks, such as Williams.¹²⁾ The effect of short side chains, such as those deliberately introduced by copolymerization with butene-1, is to introduce defects which disrupt the perfection of the crystal structure, reduce the crystallinity, and reduce the regular chain folding, thereby increasing the proportion of chains which connect one crystallite with another. High molecular weight also increases the proportion of intercrystalline links by raising the probability of a single molecule being involved in two different crystallites.

Better characterization of both long- and short-chain branching is needed. Long-chain branching, if present, could be detected by a combination of absolute molecular weight determinations by light scattering and apparent molecular weight determination by gel permeation chromatography. Long-chain branching causes a sizeable reduction in the dimensions of the polymer molecule in solution, thus reducing the apparent molecular weight by the GPC method but not affecting the light scattering results.

For short-chain branching, the effect of side group content on the crystal lattice could serve as a basis for a determination. Small side groups in ethylene a copolymers are incorporated into the crystal lattice, but an increase in the lattice parameter is required to accommodate the structural defect. Wunderlich¹³⁾ reports the dependence of the a parameter on side group concentration for a variety of side groups, including methyl, ethyl, and n-propyl. Samples would have to be annealed to eliminate residual stress effects, but, in principle, precise measurements by X-ray diffraction could be used to determine comonomer content in the range of 0% to 10%. The procedure would have the advantage of being quite straightforward and free from interferences.

Finally, the specification of polymer melt index in MIL-P-51431(EA) is not sufficient to control the polymer properties. First of all, the range in the specification, melt flow = 1.0 to 2.0, allows a great deal of latitude; the industry is capable

12. WILLIAMS, D. J. *Polymer Science and Engineering*. Prentice-Hall, Englewood Cliffs, New Jersey, 1971, p. 185.
13. WUNDERLICH, B. *Macromolecular Physics*. Academic Press, New York, v. 1, 1973, p. 153-154.

of tighter control. Second, a great deal of variation in number average molecular weight M_n is possible at a fixed melt index value, since melt viscosity is controlled by the weight-average molecular weight M_w instead. Since the ratio M_w/M_n can vary with changes in the shape of the molecular weight distribution, control of M_w does not assure control of M_n . The number average value M_n is more critical than M_w in terms of environmental attack since M_n governs the thermodynamic solution properties of the polymer, such as osmotic pressure and swelling behavior. Advances in instrumentation, particularly in gel permeation chromatography, have rendered the determination of M_w and M_n a routine measurement. It should be possible, either now or in the near future, to require specification of polyethylene by M_w and/or M_n as well as by melt index.

Alternate processes for producing a polyethylene container could result in lower and more consistent residual strain. Rotational molding, in which a polymer powder melts and then conforms to the interior shape of a heated rotating mold, is particularly attractive from this point of view. Injection molding offers the possibility of better control over residual stress strain than does extrusion, but would not necessarily eliminate residual strain entirely. As the very viscous polymer melt flows in such a mold from gate to vent, residual strain can develop, particularly at high flow rates and fast quenching conditions. Since industry practice is to maximize output rate within the constraints of the process, good quality control would be needed to keep residual strain within acceptable limits.

RECOMMENDATIONS

1. Develop a quality control specification of polymer by molecular weights M_n and M_w as measured by gel permeation chromatography, to include a minimum $M_n = 23,000$.
2. Investigate alternate processing methods, such as rotational molding or injection molding, through which residual strain in the container wall can be minimized.
3. Storage of filled containers in an upright position to minimize liquid contact with the burst plate.
4. Investigation of stress-relieving the polymer tubes at 100°C prior to fabrication.
5. Exploration of methods of fluorination of the interior surface of the DF containers.
6. Determination of absolute M_w by light scattering to provide, in conjunction with GPC data, a measure of long-chain branching.
7. Development of a method for determination of side chain content from measurement of the crystal lattice parameter a .
8. Studies of exposed polymer surface by ESCA (Electron Spectroscopy for Chemical Analysis) to determine the types of chemical bonds present, with particular regard to detecting reaction products of DF and Santonox R.
9. Characterization of alternate polyethylene resins as possible replacements for the Marlex M407MQ used in the past.

ACKNOWLEDGMENTS

The author wishes to acknowledge the invaluable contributions of the following personnel at the Army Materials and Mechanics Research Center, without whose assistance this work would not have been possible: Mr. Abram O. King, for scanning electron microscopy; Dr. Gary L. Hagnauer and Mr. David Dunn, for gel permeation chromatography; Mr. Eli Pattie and Mr. Seth Ghiorse, for mechanical testing; Dr. Robert E. Sacher and Ms. Jenny Libby, for infrared spectroscopy; and Mr. Charles Dady, for X-ray fluorescence spectroscopy.

DISTRIBUTION LIST

No. of Copies	To
1	Office of the Under Secretary of Defense for Research and Engineering, The Pentagon, Washington, DC 20301
12	Commander, Defense Technical Information Center, Cameron Station, Building 5, 5010 Duke Street, Alexandria, VA 22314
1	Metals and Ceramics Information Center, Battelle Columbus Laboratories, 505 King Avenue, Columbus, OH 43201
1	Deputy Chief of Staff for Research, Development, and Acquisition, Headquarters, Department of the Army, Washington, DC 20301 ATTN: DAMA-ARZ
1	Commander, Army Research Office, P.O. Box 12211, Research Triangle Park, NC 27709 ATTN: Information Processing Office
1	Commander, U.S. Army Materiel Development and Readiness Command, 5001 Eisenhower Avenue, Alexandria, VA 22333 ATTN: DRCLDC
1	Commander, U.S. Army Materiel Systems Analysis Activity, Aberdeen Proving Ground, MD 21005 ATTN: DRXSY-MP, H. Cohen
1	Commander, U.S. Army Electronics Research and Development Command, Fort Monmouth, NJ 07703 ATTN: DELSD-L
1	DELSD-E
1	Commander, U.S. Army Missile Command, Redstone Arsenal, AL 35809 ATTN: DRSMI-RKP, J. Wright, Bldg. 7574
4	DRSMI-TB, Redstone Scientific Information Center
1	DRSMI-RLM
1	Technical Library
2	Commander, U.S. Army Armament Research and Development Command, Dover, NJ 07801 ATTN: Technical Library
1	DRDAR-SCM, J. D. Corrie
1	DRDAR-LCA, Mr. Harry E. Peibly, Jr., PLASTECH, Director
1	DRDAR-QAC-E
1	Commander, U.S. Army Natick Research and Development Laboratories Natick, MA 01760 ATTN: Technical Library
1	Commander, U.S. Army Satellite Communications Agency, Fort Monmouth, NJ 07703 ATTN: Technical Document Center

No. of Copies	To
1 2	Commander, U.S. Army Tank-Automotive Command, Warren, MI 48090 ATTN: DRSTA-RKA DRSTA-UL, Technical Library
1	Commander, White Sands Missile Range, NM 88002 ATTN: STEWS-WS-VT
1	President, Airborne, Electronics and Special Warfare Board, Fort Bragg, NC 28307 ATTN: Library
1	Director, U.S. Army Ballistic Research Laboratory, Aberdeen Proving Ground, MD 21005 ATTN: DRDAR-TSB-S (STINFO)
1	Commander, Dugway Proving Ground, Dugway, UT 84022 ATTN: Technical Library, Technical Information Division
1	Commander, Harry Diamond Laboratories, 2800 Powder Mill Road, Adelphi, MD 20783 ATTN: Technical Information Office
1 1 1 1	Chief, Benet Weapons Laboratory, LCWSL, USA ARRADCOM, Watervliet, NY 12189 ATTN: DRDAR-LCB-TL Dr. T. Davidson Mr. D. P. Kendall Mr. J. F. Throop
1	Commander, U.S. Army Foreign Science and Technology Center, 220 7th Street, N.E., Charlottesville, VA 22901 ATTN: Military Tech, Mr. Marley
1	Commander, U.S. Army Aeromedical Research Unit, P.O. Box 577, Fort Rucker, AL 36360 ATTN: Technical Library
1	Director, Eustis Directorate, U.S. Army Air Mobility Research and Development Laboratory, Fort Eustis, VA 23604 ATTN: Mr. J. Robinson, DAVDL-E-MOS (AVRADCOM)
1	U.S. Army Aviation Training Library, Fort Rucker, AL 36360 ATTN: Building 5906-5907
1	Commander, U.S. Army Agency for Aviation Safety, Fort Rucker, AL 36362 ATTN: Technical Library
1	Commander, USACDC Air Defense Agency, Fort Bliss, TX 79916 ATTN: Technical Library
1	Commander, U.S. Army Engineer School, Fort Belvoir, VA 22060 ATTN: Library

No. of Copies	To
1	Commander, U.S. Army Engineer Waterways Experiment Station, Vicksburg, MS 39180 ATTN: Research Center Library
1	Commander, U.S. Army Environmental Hygiene Agency, Edgewood Arsenal, MD 21010 ATTN: Chief, Library Branch
1	Technical Director, Human Engineering Laboratories, Aberdeen Proving Ground, MD 21005 ATTN: Technical Reports Office
1	Commandant, U.S. Army Quartermaster School, Fort Lee, VA 23801 ATTN: Quartermaster School Library
1	Commander, U.S. Army Radio Propagation Agency, Fort Bragg, NC 28307 ATTN: SCCR-2
1	Naval Research Laboratory, Washington, DC 20375 ATTN: Dr. J. M. Krafft - Code 5830
2	Dr. G. R. Yoder - Code 6384
1	Chief of Naval Research, Arlington, VA 22217 ATTN: Code 471
2	Commander, U.S. Air Force Wright Aeronautical Laboratories, Wright-Patterson Air Force Base, OH 45433
1	ATTN: AFWAL/MLSE, E. Morrissey
1	AFWAL/MLC
1	AFWAL/MLLP, M. Forney Jr.
1	AFWAL/MLBC, Mr. Stanley Schulman
1	National Aeronautics and Space Administration, Washington, DC 20546 ATTN: Mr. B. G. Achhammer
1	Mr. G. C. Deutsch - Code RW
1	National Aeronautics and Space Administration, Marshall Space Flight Center, Huntsville, AL 35812
1	ATTN: R. J. Schwinghammer, EH01, Dir, M&P Lab
1	Mr. W. A. Wilson, EH41, Bldg. 4612
1	Ship Research Committee, Maritime Transportation Research Board, National Research Council, 2101 Constitution Ave., N. W., Washington, DC 20418
1	Librarian, Materials Sciences Corporation, Blue Bell Campus, Merion Towle House, Blue Bell, PA 19422
1	Panametrics, 221 Crescent Street, Waltham, MA 02154 ATTN: Mr. K. A. Fowler
1	The Charles Stark Draper Laboratory, 68 Albany Street, Cambridge, MA 02139
1	Wyman-Gordon Company, Worcester, MA 01601 ATTN: Technical Library

No. of
Copies

To

1 Lockheed-Georgia Company, 86 South Cobb Drive, Marietta, GA 30063
ATTN: Materials and Processes Engineering Dept. 71-11, Zone 54

1 General Dynamics, Convair Aerospace Division, P.O. Box 748, Fort Worth, TX 76101
ATTN: Mfg. Engineering Technical Library

1 Mechanical Properties Data Center, Belfour Stulen Inc., 13917 W. Bay Shore Drive,
Traverse City, MI 49684

1 Dr. Robert S. Shane, Shane Associates, Inc., 7821 Carrleigh Parkway,
Springfield, VA 22152

1 Mr. R. J. Zentner, EAI Corporation, 198 Thomas Johnson Drive, Suite 16,
Frederick, MD 21701

Director, Army Materials and Mechanics Research Center, Watertown, MA 02172

2 ATTN: DRXMR-PL

1 Author

DATE
L MED
8